Characterization of YSZ-YST Composites for SOFC Anodes

Hongpeng He, Yingyi Huang, John M. Vohs and Raymond J. Gorte
Department of Chemical & Biomolecular Engineering
University of Pennsylvania
Philadelphia, PA 19104 USA

Abstract

Porous composites of $Sr_{0.88}Y_{0.08}TiO_{3-\delta}$ (YST) and yttria-stabilized zirconia (YSZ) were formed by tape-casting methods and examined as potential anodes for SOFC. Even after calcination to 1773 K, the YSZ and YST crystallites remain as separate phases, as demonstrated by XRD and SEM with EDX analysis. Furthermore, it was possible to fabricate anode-supported electrolytes by calcination of a bilayer tape formed by casting a thin YSZ tape over the green, YSZ-YST tape. Cells with anodes having 50-wt% YST and 80-wt% YST were tested and shown to yield good open-circuit voltages, although the power densities in H_2 and CH_4 between 973 and 1173 K were modest. Impedance spectra of the cells suggest that the conductivity of the YST-YSZ composites is insufficient for high performance.

Key words: Solid oxide fuel cell, $SrTiO_3$, zirconia, anode, hydrogen, methane, SEM, tape casting

Introduction

Most research in Solid Oxide Fuel Cells (SOFC) has used Ni-based anodes [1]. While Ni anodes have demonstrated excellent performance in H_2 and syngas, they have serious limitations for direct utilization of hydrocarbons due to the fact that Ni catalyzes the formation of carbon fibers [2-5]. By using alternative conductors, such as Cu [6,7], doped ceria [8-10], and other conducting oxides [11-13], a number of groups have demonstrated that direct utilization of hydrocarbons is possible. Oxides that are electronically conductive under reducing conditions are particularly intriguing for anode applications. Unlike metallic anodes, oxides should be stable upon exposure to oxidizing conditions, an important feature for fuel cells that need to be shut down frequently. While oxides are certainly prone to sintering, one would expect oxide anodes to be more stable than metals to coarsening at high temperatures. Furthermore, oxides are generally more tolerant of impurities like sulfur than are metals.

In general, the performance of ceramic anodes tends to be poor compared to metal-containing anodes. One reason for this is almost certainly that oxides have lower electronic conductivities than metals. However, another factor is the difficulty of forming an optimized anode-electrolyte interface with ceramic anodes. For example, with Ni-cermet anodes on yttria-stabilized zirconia (YSZ) electrolytes, mixtures of NiO and YSZ are fired to high temperatures so as to allow the YSZ in the anode to sinter with the YSZ electrolyte, forming a seamless, high-surface-area interface between the anode and the electrolyte and also forming channels that allow ionic conduction into the electrode [14]. Finally, it has not been possible to fabricate anode-supported electrolytes with ceramic anodes, so that essentially all work with ceramic anodes has been with relatively thick electrolytes.

In this paper, we will discuss the fabrication of anode composites of YSZ and yttria-doped $SrTiO_3$ (YST) by tape-casting methods. First, we will show that there is minimal reaction between these components, even at a calcination temperature of 1773 K. Second, we will show that we can fabricate anode-supported, YSZ electrolytes with a wide range of YSZ-YST compositions. While the performance of cells made these composites was relatively poor due to the low electronic conductivity that we were able to achieve, there are indications that one could use this approach to fabricate high-performance SOFC.

Experimental

The YST ($Sr_{0.88}Y_{0.08}TiO_{3-\delta}$) used in this study was synthesized by first mixing stoichiometric quantities of $Sr(NO_3)_2$ (99.0%, Alfa Aesar), $Y(NO_3)_3 \cdot 6H_2O$ (99.9%, Alfa Aesar)

and TiO_2 (99.9%, Alfa Aesar) in deionized water. After drying, the powder was heated overnight in air at 1273 K, ground, and finally sintered in air at 1773 K for 4 h. X-ray diffraction (XRD) measurements demonstrated that the YST powder had the correct, perovskite structure. The YSZ was an 8-mol% Y_2O_3-stabilized zirconia (TZ-8T 8% Y) obtained from Tosoh Corporation.

Porous YST-YSZ composites with a range of compositions were prepared by tape casting, using methods similar to those used in making NiO-YSZ composites [15,16]. In this paper, the composites will be designated by the weight percent YST in the composite (e.g., The 50-wt% YST-YSZ composite will be referred to as YST50.). After adding distilled water, a dispersant (Duramax 3005, Rohm & Haas), binders (HA12 and B1000, Rohm & Haas), and pore formers (graphite and polymethyl methacrylate) to physical mixtures of YSZ and YST, the resulting slurry was cast into tapes that produced ceramic wafers, 600 μm in thickness. The porosity of all the ceramic wafers after calcination in air at 1773 K was approximately 60%, as measured by water uptake measurements [15].

To prepare fuel cells from the YST-YSZ composites, a second tape, made from pure YSZ and without pore formers, was cast directly onto the green YST-YSZ tapes described above. The YSZ layer was targeted to have a thickness of 60 μm. After calcining the two-layer tape in air to 1773 K, a 50-wt% YSZ and LSM ($La_{0.8}Sr_{0.2}MnO_3$, Praxair Surface Technologies) mixture, with 10 wt% graphite added as a pore former, was applied to the dense, YSZ side of the ceramic wafer as a paste, then calcined in air at 1523 K to form the cathode. In most cells, the porous, YST-YSZ layer was impregnated with an ethanol solution of $(NH_4)_2Ce(NO_3)_6$ and reduced in H_2 at 723 K to incorporate 10-wt% ceria as a catalyst [17]. Electronic contacts were formed using Pt mesh and Pt paste at the cathode and a Au wire with Au paste at the anode.

Each cell, having a cathode area of *ca.* 0.35 cm^2, was sealed onto 1.0-cm alumina tubes using Au paste and a ceramic adhesive (Aremco, Ultra-Temp 516). The entire cell was placed inside a furnace and heated to 973 K at 2 K/min. Dry H_2 was fed to the anode at a flow rate of 100 mL/min, while the cathode was simply left open to the air. In addition to measuring V-I curves, impedance spectra were obtained in the galvanostatic mode using a Gamry Instruments (Model EIS300), with a frequency range from 0.01 Hz to 100 kHz and using an amplitude of 3 mA/cm^2. Electrode microstructures were examined using a scanning electron microscope (SEM, JEOL JSM-6400) equipped with EDX for compositional analysis.

Results and Discussion

Because of the possibility for solid-state reactions between YST and YSZ at high temperatures, the initial experiments were aimed at characterizing the porous composites formed by tape casting mixtures of YST and YSZ. Fig. 1 shows the x-ray diffraction (XRD) pattern for pure YSZ and for YST50 (50-wt% YST-YSZ composite), prepared by tape casting, after firing to 1773 K. Compared to pure YSZ, the composite exhibits new peaks at 32, 40, 46, 57, 67, and 77 degrees 2θ, all of which can be assigned to the perovskite phase of YST. No other phases, such as strontium zirconates, were observed. Obviously, this result could still be consistent with some migration of Ti or Y between phases, or with the formation of interfacial layers too thin to observe by XRD.

We also examined the YST50 and YST80 composites using SEM with EDX analysis, with the SEM micrographs of the fractured samples shown in Fig. 2. The general appearance of the YST50 composite, shown in Fig. 2a), is very similar to that of porous YSZ wafers made using similar methods and discussed in previous publications [7,15]. The pores are interconnected, approximately 5 microns in size. A closer examination reveals that some of the crystallites are smooth, while others have small terraces. To determine the composition of the individual crystallites, EDX measurements were performed at the spots indicated on the micrograph, with the spectra shown in Fig. 3. Ignoring the Au peaks, which are due to metallization to make the sample conductive for SEM, the EDX results demonstrate that the "smooth" crystallites are YSZ and the "terraced" crystallites are YST. It is not clear whether traces of Ti have migrated into the YSZ phase. Fig. 2b), the micrograph of the YST80 sample, shows somewhat larger, "terraced" grains that can again be identified as YST, with smaller YSZ crystallites.

Fig. 4 shows V-I and power-density curves, in dry H_2 at 1073 K, for two fuel cells made with 60-μm YSZ electrolytes supported on 600-μm YST50 composites. In one case, 10-wt% ceria was added to the porous YST50 by wet impregnation. Both cells showed reasonable open-circuit voltages (OCV), greater than 1.15 V at 973K with hydrogen, implying that the YSZ electrolyte was dense and has not formed significant cracks. (Obviously, the OCV in dry H_2 also depends on the quality of the seals.) Furthermore, since any migration of Ti into the YSZ electrolyte would tend to make the YSZ electronically conductive, the excellent OCV measured on these cells demonstrates that solid-state reaction cannot have occurred on the length scale of the electrolyte. The fact that a dense YSZ electrolyte could be attached to the composite anode

was somewhat surprising since some thermal-expansion mismatch should be expected between the YSZ and YST50 layers over the very wide temperature range to which the bilayer was exposed in fabrication, 300 K to 1773 K, although an earlier report has also stated that La-doped $SrTiO_3$ has a similar CTE as YSZ [12]. The maximum power density improved significantly with the addition of ceria, increasing from 12 mW/cm^2 to 63 mW/cm^2. In other work, ceria has been shown to improve the mixed ionic and electronic conductivity [18] and to improve the catalytic activity of the anode [19]. The performance of the YST50 cell with ceria was also measured at 973 K and at 1173 K in H_2, with the performance summarized in Table 1. At both temperatures, the cell showed stable performance for 20 h, with maximum power densities of 32 mW/cm^2 at 973 K and 93 mW/cm^2 at 1173 K.

To understand the factors limiting performance of the YST50 cell with ceria, impedance spectra in Fig. 5 were measured with humidified H_2 (3% H_2O) near OCV. At each temperature, the ohmic resistances, determined by the high-frequency intercept with the real axis, were much larger than the values that would be expected for a 60-µm YSZ electrolyte, ranging from >5 $\Omega \cdot cm^2$ at 973 K to 2.3 $\Omega \cdot cm^2$ at 1173 K. By comparison, the ohmic resistance of cells from our laboratory with 60-µm electrolytes and the same cathodes, but having Cu-based anodes, was approximately 0.5 $\Omega \cdot cm^2$ at 973 K [20,21]. The obvious conclusion is that YST50 composite does not have adequate electronic conductivity. It should be noted that we did not attempt a high-temperature reduction, which previous work has shown to be necessary for achieving high conductivity in YST [12].

Fig. 6 shows the performance curves for the YST50 cell with ceria using humidified CH_4 (3% H_2O) as the fuel. Power densities of 30 and 80 mW/cm^2 were achieved at 1073 and 1173 K, values that are somewhat lower than that obtained for H_2. In agreement with previous reports with methane on ceramic anodes, the performance of the cells was stable under these conditions.

Because 50-wt% YST might not be sufficient to provide "percolation" of the YST phase for electronic conductivity, a cell was also fabricated with an anode made from YST80 and a 60-µm YSZ electrolyte, again with 10-wt% ceria added to the YST80 to enhance catalytic activity. The OCV and maximum power densities for the YST80 cell are shown in Table 1 for comparison to the YST50 cell. The YST80 cell again showed excellent OCV in H_2, demonstrating that a dense electrolyte had been obtained. However, the performance of this cell was actually slightly lower than that of the cell with YST50 as the anode. We had expected that the higher fraction of YST in the anode would improve the electronic conductivity; however, any

increase in electronic conductivity appears to have been balanced by poorer ionic conductivity or anode structure.

Conclusions

The following new observations were made in this study:

1) Mixtures of yttria-stabilized zirconia (YSZ) and yttria-doped $SrTiO_3$ (YST) can be heated to temperatures as high as 1773 K without undergoing substantial solid-state reactions.
2) Composites of these two oxides can be made by tape-casting methods. Porous structures composed of YSZ and YST crystallites can be fabricated with a wide range of compositions.
3) Dense, thin YSZ electrolytes can be attached to YST-YSZ composite anodes having YST compositions as high as at least 80-wt%. The excellent open-circuit voltages (OCV) obtained on these cells demonstrate the formation of dense electrolytes without cracks, which in turn demonstrates that YSZ and YST have a reasonably good CTE match.
4) The YST-YSZ composite anodes can be used for direct utilization of CH_4.

Acknowledgments

This work was supported by the Office of Naval Research.

References:

1) N. Q. Minh, J. Am. Ceram. Soc., 76 (1993) 563.
2) M. L. Toebes, J. H. Bitter, A. J. van Dillen, and K. P. de Jong, Catal. Today, 76 (2002) 33.
3) R. T. K. Baker, P. S. Harris, J. Henderson, R. B. Thomas, Carbon, 13 (1975) 17.
4) R. T. K. Baker, G. R. Gadsby, and S. Terry, Carbon, 13 (1975) 245.
5) C. W. Keep, R. T. K. Baker, and J. A. France, J. Catal., 47 (1977) 232.
6) S. Park, J. M. Vohs, and R. J. Gorte, Nature, 404, (2000) 265.
7) R. J. Gorte, S. Park, J. M. Vohs, and C. Wang, Adv. Mater. 12 (2000) 1465.
8) E. S. Putna, J. Stubenrauch, J. M., Vohs, and R. J. Gorte, Langmuir 11 (1995) 4832.
9) B. C. H. Steele, I. Kelly, P. H. Middleton, and R. Rudkin, Solid State Ionics, 28 (1988) 1547.
10) O. A. Marina, C. Bagger, S. Primdahl, and M. Mogensen, Solid State Ionics, 123 (1999) 199.
11) J. T. S. Irvine and A. Sauvet, Fuel Cells, 1 (2001) 205.
12) O. Marina, N. L. Canfield, and J. W. Stevenson, Solid State Ionics, 149 (2002) 21.
13) J. Liu, B. D. Madsen, Z. Q. Ji, and S. A. Barnett, Electrochem. Sol. St. Lett., 5 (2002) A122.
14) A.V. Virkar, J. Chen, C.W. Tanner, and J-W Kim, Solid State Ionics, 131 (2000) 189.
15) M. Boaro, J. M. Vohs, R. J. Gorte, J. Am. Ceram. Soc., 86, (2003) 395.
16) H. Kim, C. daRosa, M. Boaro, J. M. Vohs, and R. J. Gorte, J. Am. Ceram. Soc., 85 (2002) 1473.
17) H. P. He, J. M. Vohs, R. J. Gorte, J. Electrochem. Soc., 150 (2003) A1470.
18) E. Perry Murray, M. J. Sever, and S. A. Barnett, Solid State Ionics, 148 (2002) 27.
19) S. McIntosh, J. M. Vohs, and R. J. Gorte, Electrochimica Acta, 47 (2002) 3815.
20) S. McIntosh, J. M. Vohs, and R. J. Gorte, J. Electrochem. Soc., 150 (2003) A470.
21) S. McIntosh, J. M. Vohs, and R. J. Gorte, J. Electrochem. Soc., 150 (2003) A1305.

Figure Captions:

Fig. 1 XRD patterns of YSZ and the 50-wt% YST-YSZ composite formed by tape-casting methods. The results indicate that there is no solid-state reaction between YSZ and YST, even after calcination to 1773 K for 4 h.

Fig. 2 SEM micrographs of fracture of the composites made from a) 50 wt% YST (YST50) and b) 80 wt% YST (YST80).

Fig. 3 Results from EDX analysis for selected spots on the micrographs in Fig. 2.

Fig. 4 Performance curves in dry H_2 at 1073 K for cells having a YST50 anode, with and without the addition of 10-wt% ceria.

Fig. 5 Impedance spectra for the cell having a YST50 anode with 10-wt% ceria, using humidified H_2. The spectra were taken near OCV as a function of temperature.

Fig. 6 Performance curves in humidified CH_4 for the cell having a YST50 anode with 10-wt% ceria as a function of temperature.

Table I Summary of the performance data for the fuel cells made with YST50 and YST80 composite anodes using dry H_2 and humidified CH_4 as fuels. The power densities are given as mW/cm^2, while the values in parenthesis are the open-circuit voltages.

Temperature	YST50		YST80	
	H_2	CH_4	H_2	CH_4
973K	31 (1.195)		23 (1.174)	
1073K	62 (1.165)	35 (1.01)	48 (1.167)	20 (1.057)
1173K	95 (1.143)	78 (1.05)	74 (1.132)	48 (1.083)

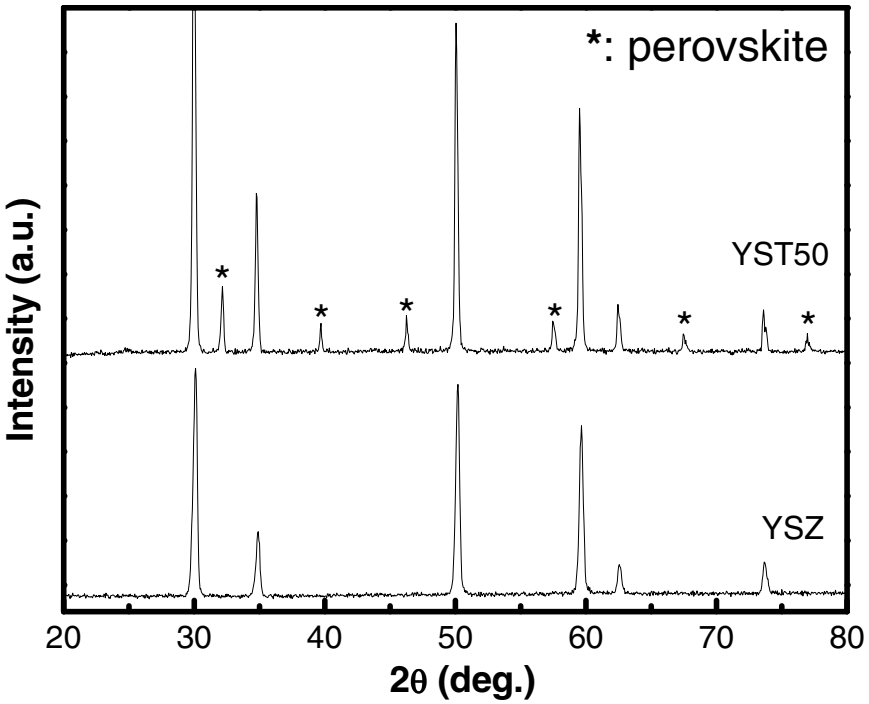

Fig. 1

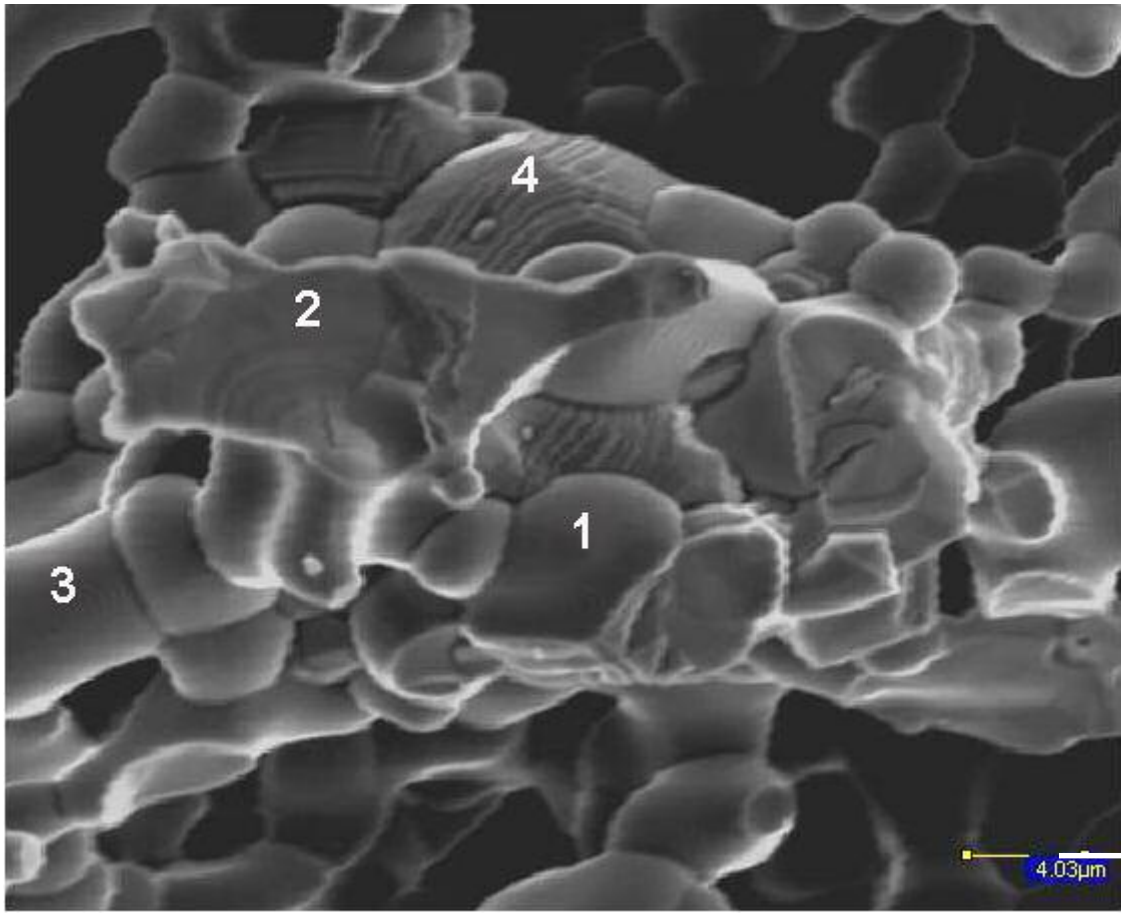

4µm

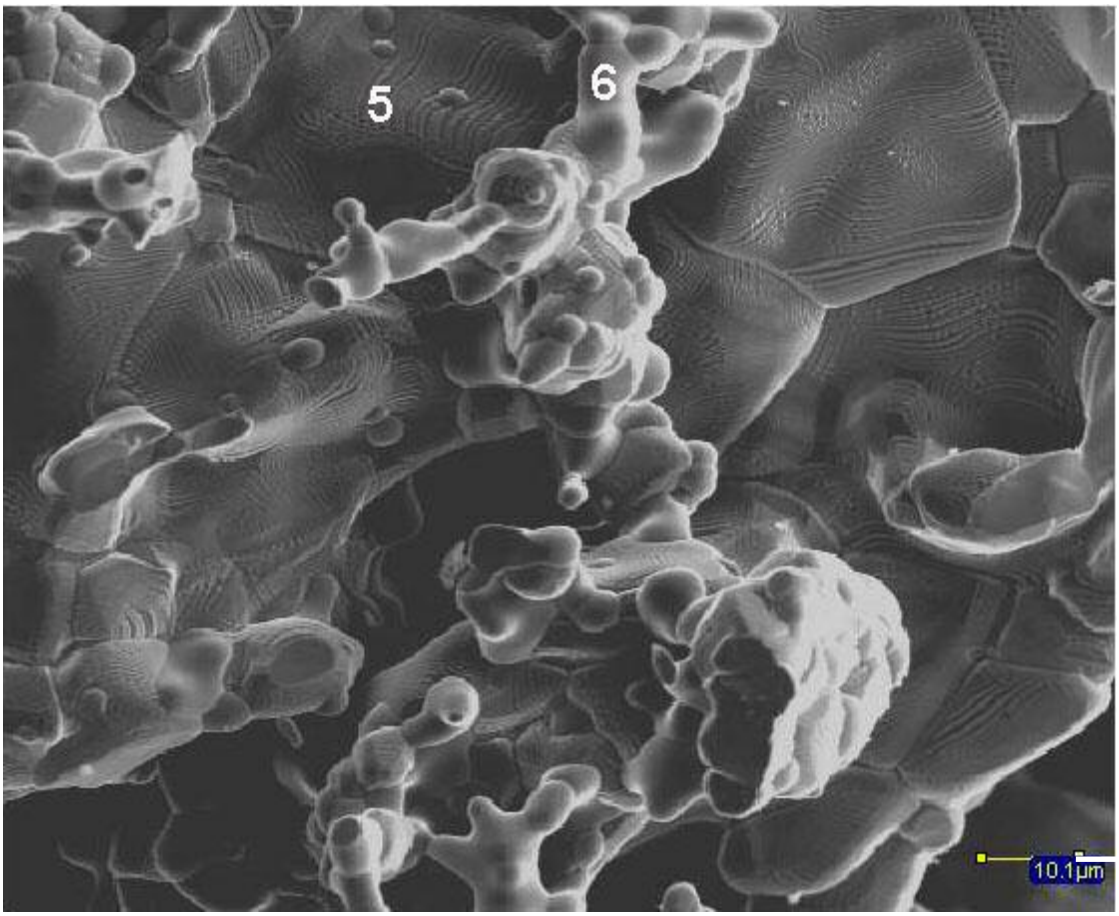

10µm

Fig. 2

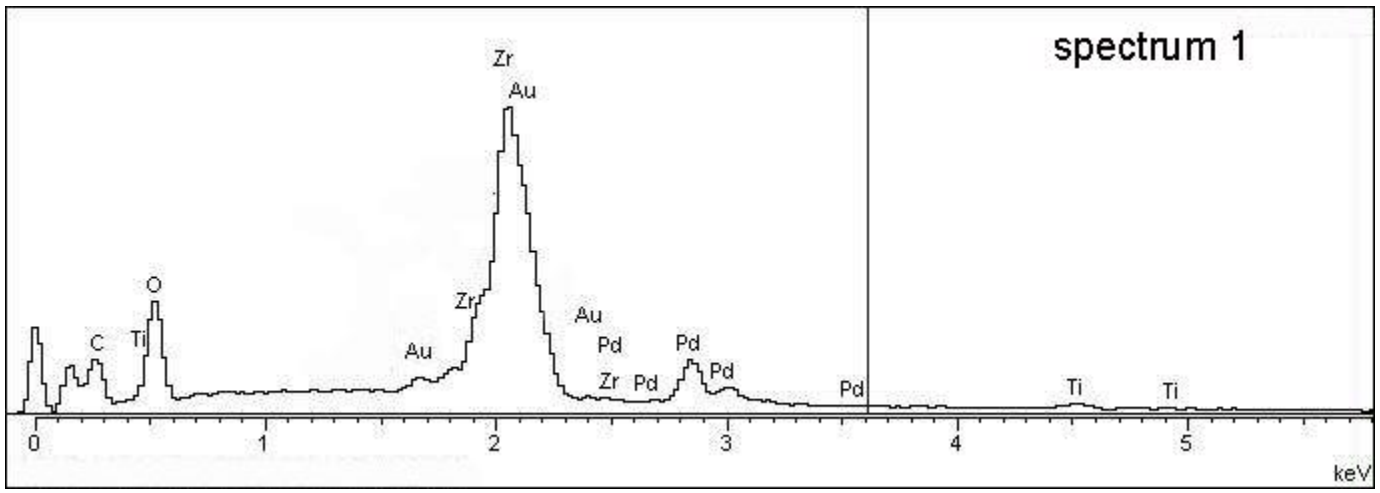
spectrum 1
Zr
Au
O
C
Ti
Au
Zr
Au
Pd
Zr
Pd
Pd
Pd
Pd
Ti
Ti
0
1
2
3
4
5
keV

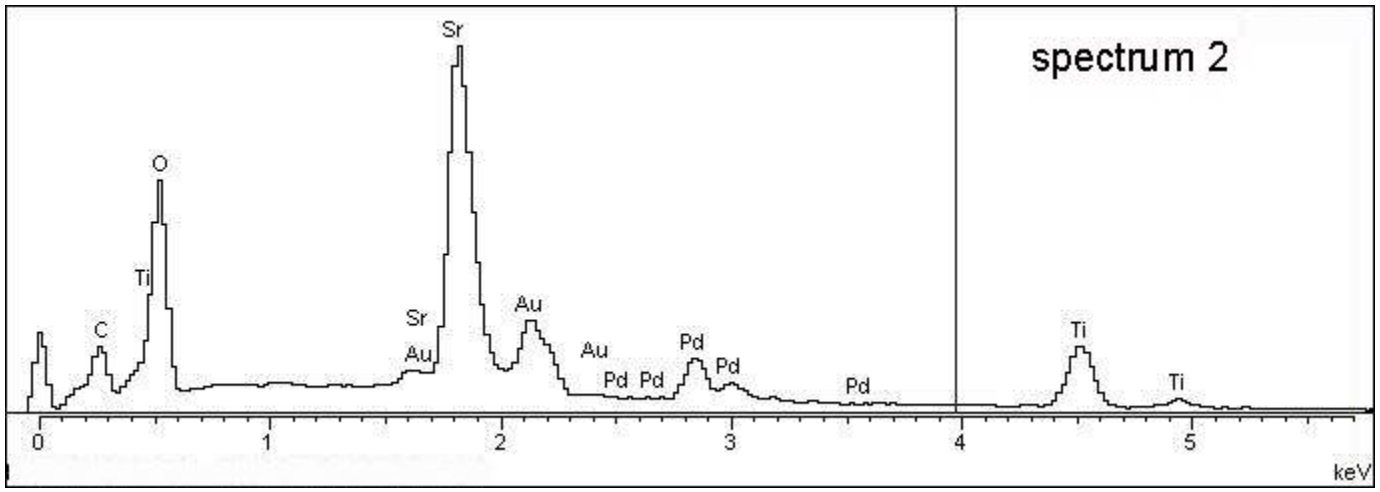
spectrum 2
Sr
O
Ti
C
Sr
Au
Au
Au
Pd
Pd
Pd
Pd
Pd
Ti
Ti
0
1
2
3
4
5
keV

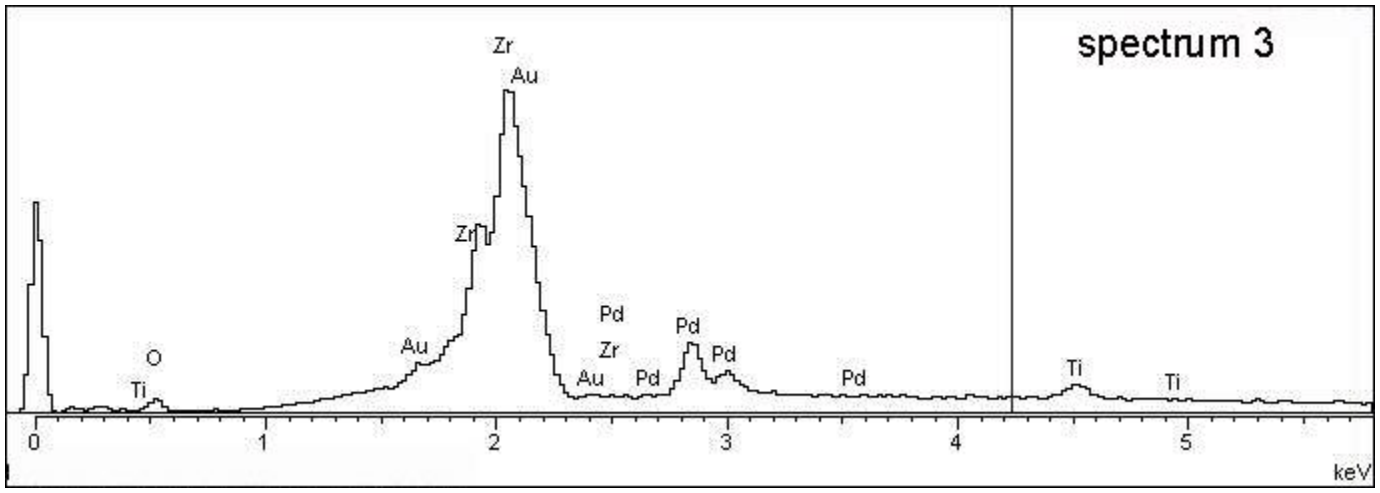
spectrum 3
Zr
Au
Zr
O
Ti
Au
Pd
Zr
Au
Pd
Pd
Pd
Pd
Ti
Ti
0
1
2
3
4
5
keV

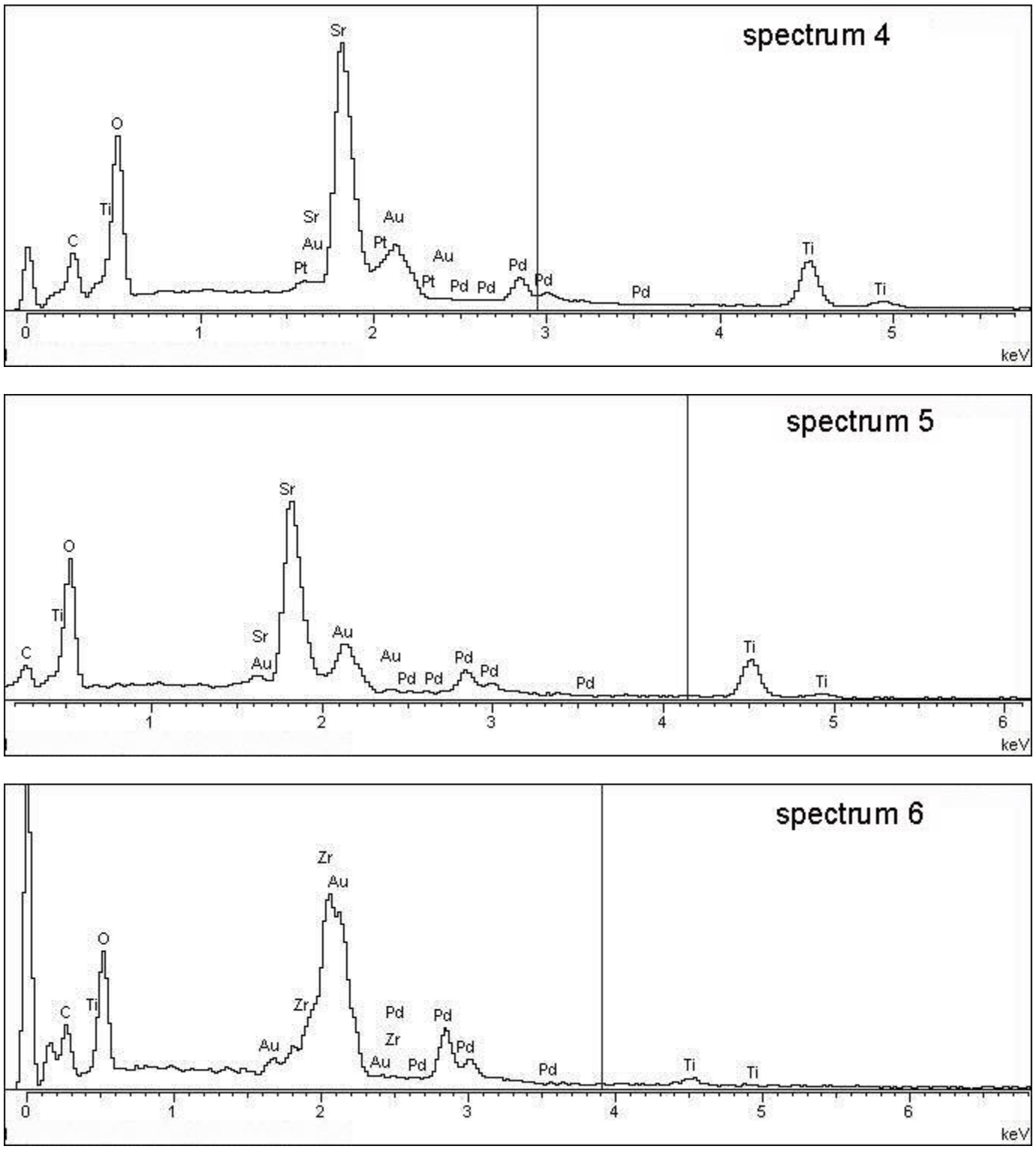
spectrum 4
Sr
O
Ti
C
Sr
Au
Pt
Au
Pt
Au
Pt
Pd
Pd
Pd
Pd
Pd
Ti
Ti
0
1
2
3
4
5
keV
spectrum 5
Sr
O
Ti
C
Sr
Au
Au
Au
Pd
Pd
Pd
Pd
Pd
Ti
Ti
1
2
3
4
5
6
keV
spectrum 6
Zr
Au
O
C
Ti
Zr
Au
Pd
Zr
Au
Pd
Pd
Pd
Pd
Ti
Ti
0
1
2
3
4
5
6
keV

Fig. 3

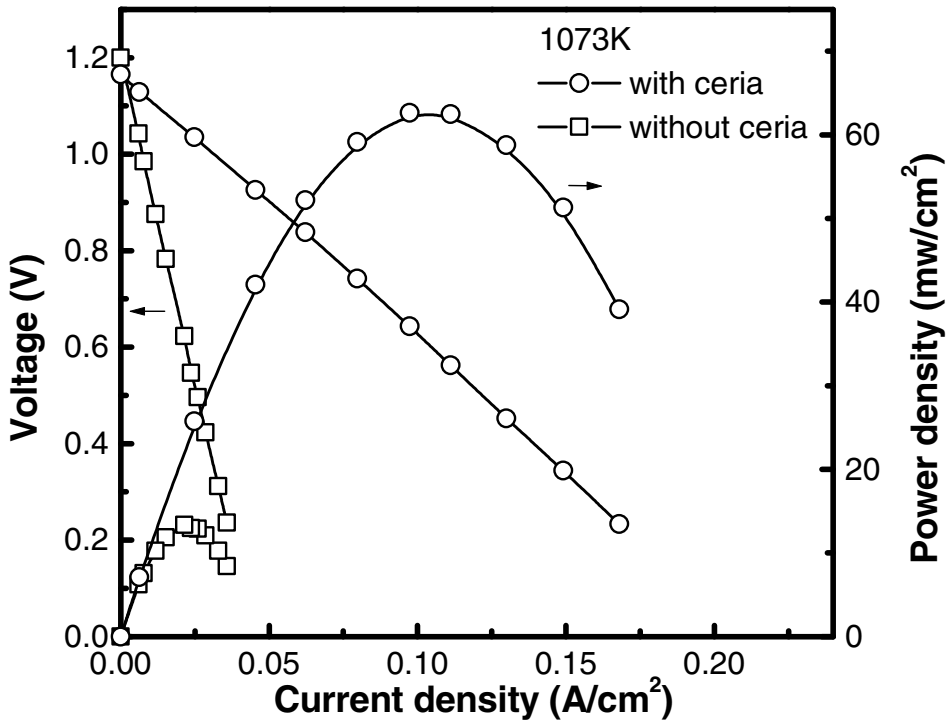
1073K
with ceria
without ceria
Voltage (V)
Power density (mw/cm^2)
Current density (A/cm^2)
0.0
0.2
0.4
0.6
0.8
1.0
1.2
0
20
40
60
0.00
0.05
0.10
0.15
0.20

Fig. 4

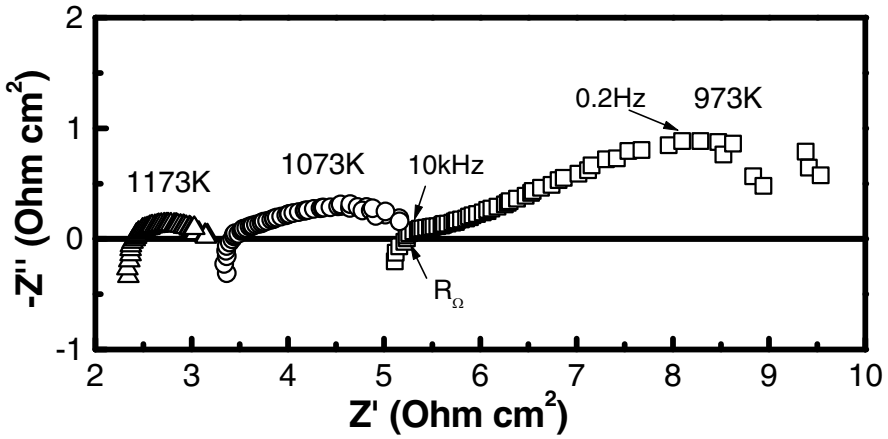
-Z'' (Ohm cm2)
Z' (Ohm cm2)
1173K
1073K
10kHz
0.2Hz
973K
RΩ

Fig. 5

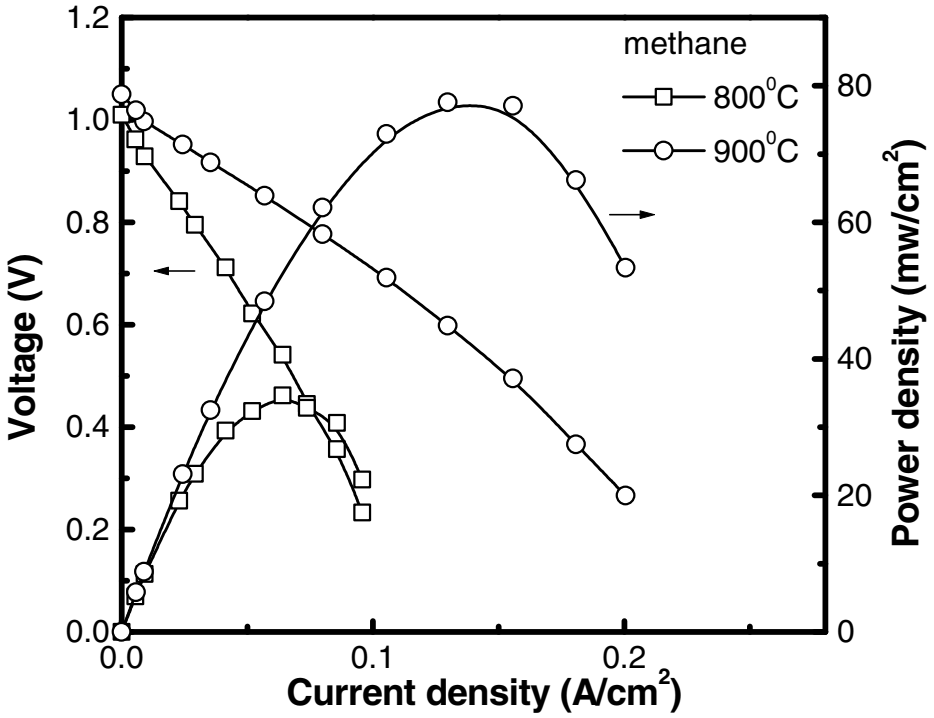
methane
800°C
900°C
Voltage (V)
Power density (mw/cm2)
Current density (A/cm2)

Fig. 6